Advances in Geo-Energy Research

Vol. 13, No. 3, p. 169-175, 2024

Short communication

Stability analysis of surrounding rock of multi-cavern for compressed air energy storage

Wendong Ji[1]*, Shu Wang[2], Jifang Wan[1], Shaozhen Cheng[1], Jiaxin He[1], Shaohua Shi[1]

[1]*China Energy Digital Technology Group Co., Ltd., Beijing 100044, P. R. China*

[2]*School of Civil and Architectural Engineering, Beijing Jiaotong University, Beijing 100044, P. R. China*

Keywords:
Compressed air energy storage
working pressure
cavern type
pillar space
cavern diameter

Cited as:
Ji, W., Wang, S., Wan, J., Cheng, S., He, J., Shi, S. Stability analysis of surrounding rock of multi-cavern for compressed air energy storage. Advances in Geo-Energy Research, 2024, 13(3): 169-175.
https://doi.org/10.46690/ager.2024.09.03

Abstract:
Compressed air energy storage in artificial caverns can mitigate the dependence on salt cavern and waste mines, as well as realize the rapid consumption of new energy and the "peak-cutting and valley-filling" of the power grid. At the same time, the safety and stability of the surrounding rock of gas storage has attracted extensive attention. Based on finite element simulation, a numerical model of shallow-buried double-chamber for compressed air energy storage is established, and the influence of working pressure, cavern type, pillar space, and cavern diameter on the mechanical behavior of surrounding rock is analyzed. It is discovered that the cavern type significantly affects the response of the surrounding rock, whose deformation and plastic strain in the horseshoe-shaped cavern is significantly larger than that in the circular cavern. For circular caverns, the pillar space of 2∼3 times the cavern diameter is only suitable for low working pressure, and the plastic strain and deformation of surrounding rock increases sharply with the increase of working pressure. It is more appropriate to select the pillar space that is 4 times the cavern diameter when the working pressure is greater than 16 MPa. With the increase in the cavern diameter, the maximum deformation of the surrounding rock accelerates rapidly.

1. Introduction

The technology of compressed air energy storage uses compressed air as a medium to store energy and generate electricity. This strategy uses redundant or unstable electric energy to drive the compressor, which compresses the air in multiple stages and stores it in the underground cavity. When necessary, the compressed air stored underground is pumped into the turbine and the stable electric energy is output through the generator. Compressed air energy storage has the advantages of high efficiency, small land occupation, flexible operation, and low investment cost; therefore, it has developed rapidly around the world in recent years (Marcus et al., 2016; Jafarizadeh et al., 2020; Wan et al., 2023). At present, the main forms of underground gas storage include the geological structures of oil storage and gas storage, salt caverns, underground aquifers, and artificial caverns excavated in hard rocks (Wan et al., 2024). The first three types all depend on special geological structures, and are limited in terms of the location of gas storage. In contrast, the excavation of artificial caverns in hard rock is not limited to specific geological structures, and its site selection is more flexible (Zimmels et al., 2002; Lund and Salgi, 2009; Kim et al., 2021; Wang et al., 2022; Peng et al., 2023).

The safety and stability of the surrounding rock is the key to ensure the long-term safe operation of the compressed air energy storage power station. Thus far, several studies on the mechanical response of surrounding rock of single-cavern gas storage have been conducted (Kushnir et al., 2012; Rutqvist et al., 2012; Serbin et al., 2015; Leis, 2021). Based on Laplace transform and the superposition principle, Zhou et al. (2015) analyzed the influence of temperature and gas pressure during compressed air energy storage on the stress and displacement of surrounding rock by means of a thermo-elastic axisymmetric model. With the aid of finite element numerical simulation, Xia et al. (2014) analyzed the distri-

Yandy Scientific Press

*Corresponding author.
E-mail address: wdji5151@ceec.net.cn (W. Ji); w17393182004@163.com (S. Wang); wanjifang@126.comm (J. Wan); szcheng2937@ceec.net.cn (S. Cheng); jxhe7219@ceec.net.cn (J. He); shshi7373@ceec.net.cn (S. Shi).

Received May 21, 2024; revised June 4, 2024; accepted June 16, 2024; available online June 19, 2024.

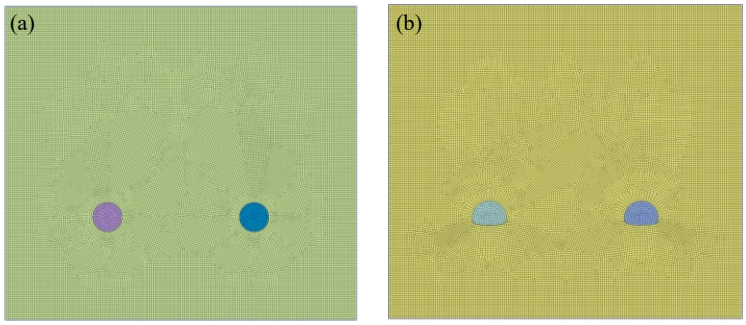

Fig. 1. Schematic diagram of the proposed model. (a) Circular cavern and (b) horseshoe-shaped cavern.

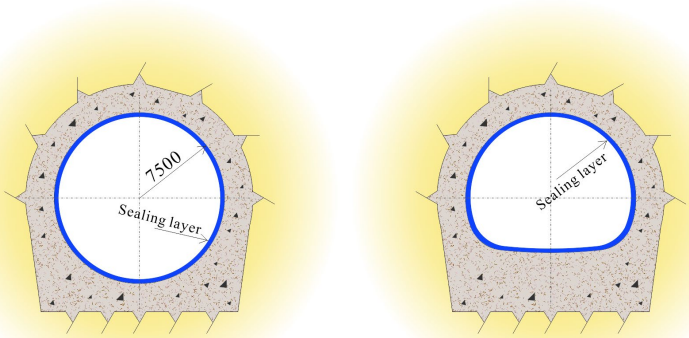

Fig. 2. Circular and horseshoe-shaped cavern.

bution law of plastic zone and strain of surrounding rock of compressed air energy storage caverns under the condition of high internal pressure, and obtained the reasonable form of gas storage. Through the cyclic loading test of scaled test cavern, Jiang et al. (2020) revealed the working mechanism of sealing layer, concrete lining and surrounding rock of artificial cavern gas storage under high internal pressure, which provided valuable experience for the design of single cavern gas storage. However, with the gradual increase in the scale of compressed air energy storage power stations, gas storage is often composed of multiple caverns. In this case, the interaction between caverns will greatly influence the stability of the surrounding rock. However, there is little research on the mechanical response of surrounding rock of multi-chamber gas storage.

In this work, numerical simulation is carried out to explore the influence of pillar space and working pressure on the mechanical behavior of surrounding rock of gas storage, and the appropriate pillar space under different working pressures is obtained. By comparing the deformation and plastic strain of surrounding rock between a circular cavern and a horseshoe-shaped cavern, the cavern type suitable for shallow gas storage is determined. In addition, the influence of cavern diameter on the mechanical response of surrounding rock is analyzed and summarized. The research results can provide a valuable reference for the design and construction of multi-chamber gas storage.

2. Numerical model and parameters

2.1 Numerical model

Taking the longitudinal center section of gas storage as the research object, a two-dimensional numerical calculation model, shown in Fig. 1, is established by a finite element program. The gas storage is composed of two parallel caverns with the same shape and size. To eliminate the boundary effect, the distance from the gas storage boundary to the model boundary is 3 times the cavern diameter (TCD), and the buried depth of the cavern is 100 m. Taking the case that the pillar space is 4 TCD as an example, the width and height of the numerical model are 180 m and 160 m, respectively. Fixed constraints and normal constraints are imposed on the bottom and two sides of the model, respectively, and the top of the model is a free surface.

As shown in Fig. 2, the gas storage consists of circular caverns or horseshoe-shaped caverns. The diameter of the circular cavern is 15 m. To ensure that the cross-sectional areas of circular cavern and horseshoe-shaped cavern are equal, the width of horseshoe-shaped cavern is 18 m. In the numerical simulation, the distance between the two caverns is set as 2 times, 3 times and 4 TCD, respectively, and the working pressure of the caverns is taken as 12, 15 and 18 MPa, respectively.

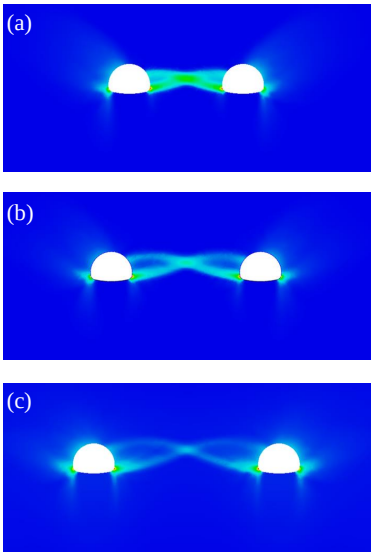

Fig. 3. Plastic strain of horseshoe-shaped cavern with different pillar spaces. (a) 2, (b) 3 and (c) 4 TCD.

2.2 Parameters

The gas storage of the artificial cavern is mainly composed of sealing layer, high-performance concrete lining and surrounding rock, where the surrounding rock mainly bears the expansion pressure generated by indoor high-pressure gas, and the sealing layer and concrete lining cooperate with each other to ensure the sealing performance of the gas storage. In the numerical simulation, it is assumed that the gas storage has good sealing performance and the lining and sealing layer are not simulated. The pressure in the tunnel is simulated by the equivalent normal stress acting on the cavern wall. Because the gas storage is generally built in a relatively complete granite stratum, the surrounding rock is considered as a continuous medium and the Mohr-Coulomb yield criterion is adopted. The weight, elastic modulus and Poisson's ratio of the surrounding rock are 26.9 kN/m^3, 47.55 GPa and 0.21, respectively. The cohesion and internal friction angle are 2.11 MPa and 40.4°, respectively.

The main steps of numerical calculation are as follows:

1) Select the section type of the cavern, establish the calculation model, balance the initial stress, and carry out the displacement clearance treatment;
2) Passivate the artificial cavern unit to simulate its excavation process;
3) Set the corresponding construction stage for different working pressures and calculate the model respectively to make it reach a balanced state;
4) Change the pillar space and repeat steps 1)-3).

3. Results and analysis

3.1 Horseshoe-shaped cavern

When the working pressure is 18 MPa, the plastic strain nephogram of the horseshoe-shaped cavern with different pillar spaces is shown in Fig. 3. It can be seen that changing the pillar space has a great influence on the plastic strain area. When the pillar space is 2 TCD, the plastic strain area of the two caverns overlaps and the peak plastic strain of the surrounding rock is located at the arch foot, with the maximum value of 4.59×10^{-3}. With the increase in the pillar space, the overlapping area of plastic strain of the surrounding rock of two caverns decreases and the maximum plastic strain of surrounding rock also decreases gradually. When the pillar space is increased to 4 TCD, the plastic strain of surrounding rock decreases to 3.66×10^{-3}, and the overlapping area of plastic strain between the two caverns is very small, which indicates that the interaction between of the two caverns is weak. The maximum plastic strain all appears at the wall foot of the cavern regardless of the distance between the caverns, which indicates that when the horseshoe-shaped cavern is used as the compressed air energy storage, stress concentration will occur at the wall foot of the cavern, which is highly unfavorable.

The curves of plastic strain and deformation of the surrounding rock of horseshoe-shaped cavern under working pressure are exhibited in Fig. 4. It is easy to infer that with the increase in working pressure, the plastic strain and deformation of surrounding rock increases significantly. When the working pressure is 18 MPa, the plastic strain value and deformation value of surrounding rock are 3∼5 times that of 12 MPa. As shown in Fig. 4(a), with the increase in pillar space, the plastic strain of surrounding rock decreases. For example, under the working pressure of 18 MPa, the maximum plastic strain reduces by 7.63% when the pillar space increases from 2 to 3 TCD. When the pillar space increases from 2 to 4 TCD, the maximum plastic strain reduces by 20.3%. As shown in Fig. 5(b), under the condition of high working pressure, the rock deformation values decrease greatly with the increase in the pillar space. Taking the working pressure of 18 MPa as an example, when the pillar space increases from 2 to 4 TCD, the maximum deformation value decreases from 16.84 mm to 11.75 mm, constituting a decrease of 30.2%. When the working pressure is lower than 14 MPa, the results of mechanical response of the surrounding rock with pillar spaces of 3 and 4 TCD are similar. These data show that the higher the working pressure in the caverns, the larger the required pillar space.

3.2 Circular cavern

Under the working pressure of 18 MPa, the plastic strain nephograms of the circular cavern with different pillar spaces are shown in Fig. 5. It is obvious that changing the pillar space will significantly affect the plastic strain of the surrounding rock. When the pillar space is 2 TCD, the plastic strain area between the two caverns overlaps, which is consistent with the results for the horseshoe-shaped cavern. The difference is that the maximum plastic strain appears in the middle rock pillar between the two caverns, with a value of 19.2×10^{-4}. With the increase in the pillar space, the maximum plastic strain of surrounding rock decreases significantly, and the position of the maximum plastic strain also shifts from the position of the middle rock pillar to the periphery of the

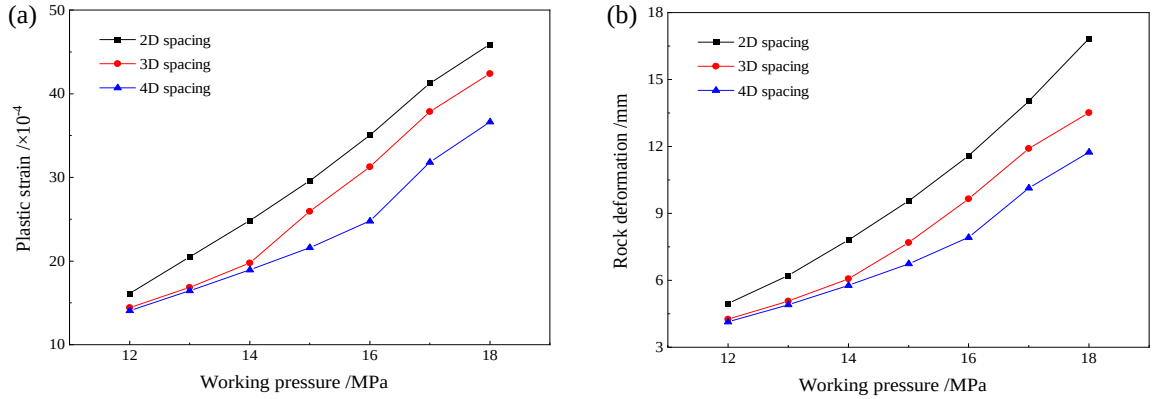

Fig. 4. Variation curve of plastic strain and deformation of horseshoe-shaped cavern under working pressure. (a) Plastic strain and (b) deformation.

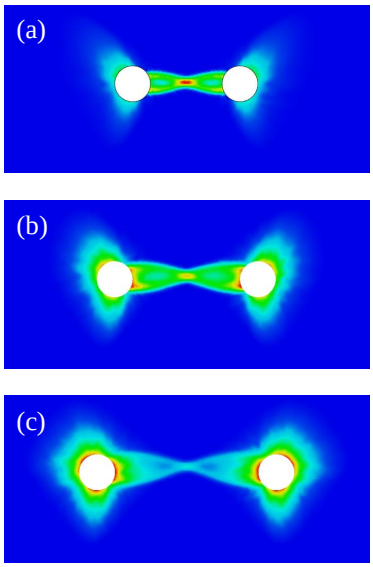

Fig. 5. Plastic strain of horseshoe-shaped cavern with different pillar spaces. (a) 2, (b) 3 and (c) 4 TCD.

caverns. When the pillar space reaches 4 TCD, the maximum plastic deformation is 5.9×10^{-4}, which is 70% lower than that for 2 TCD. Compared with the horseshoe-shaped cavern, the distribution of plastic strain of the surrounding rock of circular cavern is more discrete, which indicates that the stress concentration of surrounding rock is weak and its stress is more reasonable.

The curves of plastic strain and deformation of the surrounding rock of circular cavern under working pressure are displayed in Fig. 6. Consistent with the results for horseshoe-shaped caverns, with the increasing working pressure in the circular cavern, the plastic strain and deformation of surrounding rock are improved significantly. When the working pressure is increased from 12 to 18 MPa and the pillar space is 2 TCD, the plastic strain is increased by about 5 times. Meanwhile, when the pillar space is 4 TCD, the plastic strain is only increased by about 0.5 times. These results show that the smaller the pillar space, the more significant the effect of increasing working pressure on the mechanical response of surrounding rock. When the working pressure is lower than 16 MPa, the plastic strain values of pillar space of 3 and 4 TCD are basically the same, and the difference in rock deformation is also small. When the working pressure is greater than 16 MPa, the plastic strain area of the two caverns overlaps when the pillar space is 2 TCD, and the plastic strain is obviously greater than that when the pillar space is 3∼4 TCD. These results demonstrate that the pillar space of 2 TCD is only suitable for low working pressure. In addition, under the condition of high working pressure, increasing the pillar space can still effectively reduce the plastic strain and deformation.

Compared with the horseshoe-shaped cavern, the plastic strain and deformation of the surrounding rock of the circular cavern are obvious smaller, which shows that the circular cavern is more conducive to reducing the mechanical response of the surrounding rock. Therefore, considering the safety and stability of surrounding rock, the circular cavern is more suitable than the horseshoe-shaped cavern.

3.3 Working pressure change in right cavern

To study the mechanical behavior of surrounding rock under constant pressure of one cavern and gradually increasing the pressure of the other cavern, the working pressure of the left cavern is fixed at 18 MPa, and the surrounding rock deformation is calculated by numerical simulation when the working pressure of the right cavern is 0, 6, 9, 12, 15 and 18 MPa respectively. The calculation results are shown in Fig. 7, and the maximum rock deformation under different conditions is summarized and listed in Table 1. As shown in Fig. 7(a), when the pressure of the right cavern is 0, the surrounding rock deformation is concentrated in the side wall of the left cavern, and the surrounding rock deformation of the right sidewall is significantly greater than that of the left sidewall. With the increase in the pressure of the right cavern, the position of the maximum deformation of the surrounding rock gradually moves from the sidewall to the vault (Fig. 7(b)). When the pressure in the left cavern is further increased to 18 MPa,

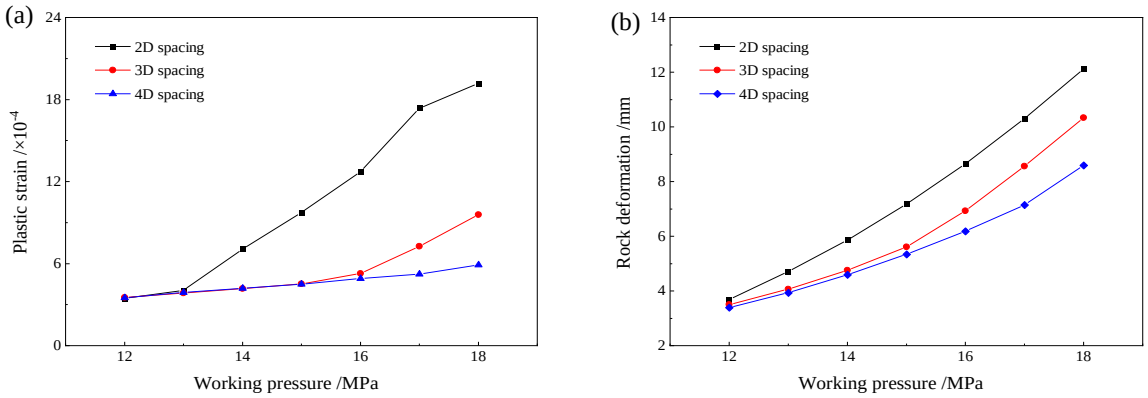

Fig. 6. Variation curve of plastic strain and deformation of circular cavern under working pressure. (a) Plastic strain and (b) deformation.

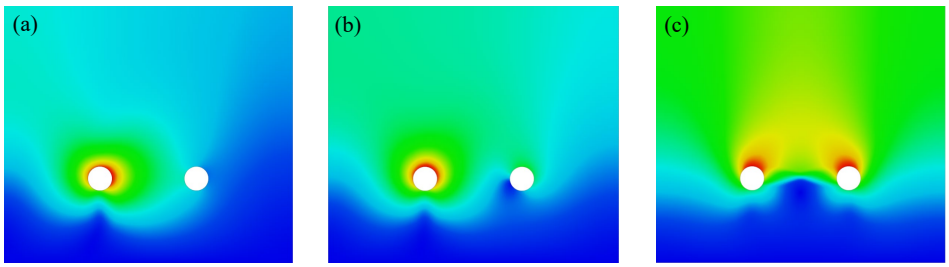

Fig. 7. Color map of cavern deformation under different working pressures. (a) 0, (b) 9 and (c) 18 MPa.

Table 1. Cavern deformation under different working pressures (mm).

Pillar space	Position	Rock deformation (mm)					
		0 MPa	6 MPa	9 MPa	12 MPa	15 MPa	18 MPa
2 TCD	Left	7.09	6.78	7.42	8.61	10.12	12.1
	Right	3.29	2.76	4.06	6.19	8.9	12.1
3 TCD	Left	6.89	6.72	6.83	7.22	8.55	10.4
	Right	2.17	2.15	3.04	4.44	7.01	10.4
4 TCD	Left	6.85	6.44	6.86	7.11	7.54	8.6
	Right	1.56	1.84	2.74	4.07	5.86	8.6

the pressure in the left and the right caverns are equal and the surrounding rock deformation of the two caverns is very close, showing a symmetrical distribution pattern.

It can be inferred from Table 1 that the deformation of rock is greatly influenced by the pillar space: with the increase in the pillar space, the rock deformation decreases rapidly. When the pillar space is increased from 2 to 4 TCD, the maximum surrounding rock deformation of the left tunnel under working pressures of 0, 6, 12 and 18 MPa decreases by 3.4%, 5.0%, 17.4% and 28.9%, respectively. As the working pressure of the left tunnel increases, the effect of increasing the pillar space to reduce the deformation of the surrounding rock becomes more obvious. When the pillar space remains unchanged, with the increase in the working pressure of the right cavern, the maximum deformation of the two caverns first decreases and then increases. This phenomenon occurs because the existence of the right cavern destroys the integrity of the stratum and enlarges the deformation of surrounding rock when the pressure of the right cavern is small. When the pressure of the right cavern exceeds the initial geostress, the surrounding rock of the right cavern expands outward, limiting the deformation of the surrounding rock of the left cavern.

3.4 Influence of cavern diameter

To explore the influence of cavern diameter on the mechanical response of the surrounding rock, three kinds of circular

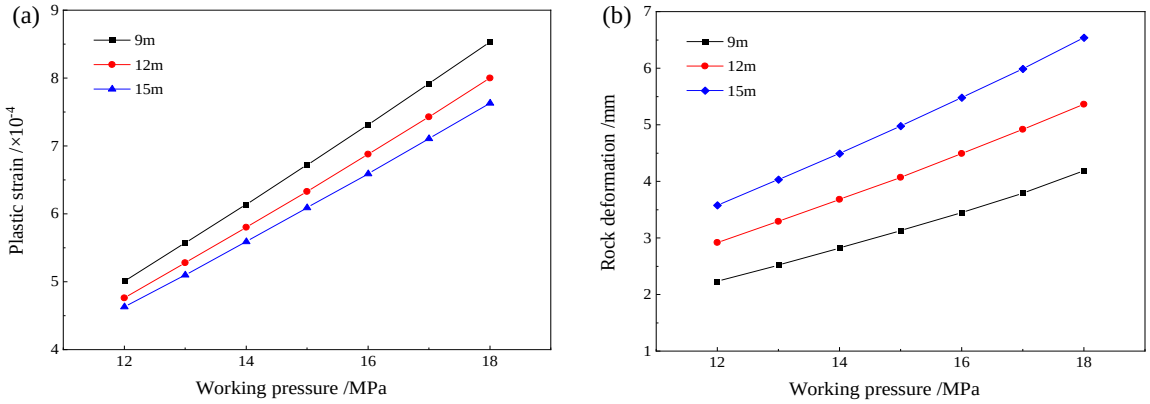

Fig. 8. Variation curves of plastic strain and deformation of circular cavern under working pressure. (a) Plastic strain and (b) deformation.

cavern with diameters of 9, 12 and 15 m are selected for comparative analysis. The variation curves of plastic strain and deformation of circular cavern under working pressure and with different cavern diameters are displayed in Fig. 8. Under the working pressure of 18 MPa, the maximum plastic strains of the surrounding rocks of circular caverns with diameters of 9, 12 and 15 m are 8.53×10^{-4}, 8.0×10^{-4} and 7.63×10^{-4} respectively. It is easy to infer that the maximum plastic strain of surrounding rock gradually decreases with the increase in cavern diameter. Compared with the former, the latter two results decrease by 6.1% and 10.5% respectively. In addition, the cavern diameter significantly affects the deformation of surrounding rock, and the rock deformation increases rapidly with increasing cavern diameter. Taking the working pressure of 18 MPa as an example, the maximum rock deformation of circular caverns with diameters of 9, 12 and 15 m are 4.19, 5.36 and 6.54 mm, respectively. Compared with the former, the latter two results are improved by 27.9% and 56.1% respectively.

Overall, with the increase in cavern diameter, the deformation of surrounding rock shows an increasing trend. From the point of view of surrounding rock stability, the diameter of gas storage cavern should be as small as possible. However, in recent years, the scale of compressed air energy storage power station has gradually expanded, which has led to a larger gas storage capacity requirement. In this case, the small diameter of the chamber will result in its length being too large, which will seriously restrict the location of the gas storage. In addition, the excessive length of the gas storage may also lead to the inhomogeneity of the temperature of the gas storage and reduce the energy storage efficiency of the compressed air energy storage power station. Therefore, it is not necessarily true that the smaller the cavern diameter of the gas storage, the better. It is important to comprehensively consider multiple factors such as site and energy efficiency, and ultimately choose a reasonable cavern diameter.

4. Conclusions

Based on finite element numerical simulation, this paper systematically studied the influence of the working pressure, cavern type, pillar space and cavern diameter of compressed air energy storage on the mechanical response of the surrounding rock. From the results, the following main conclusions could be drawn:

1) The cavern type significantly impacts the response of the surrounding rock, and the rock deformation and plastic strain in the horseshoe-shaped cavern is significantly larger than that in the circular cavern. Considering the deformation of the surrounding rock, the circular cavern is more suitable than the horseshoe-shaped cavern.
2) For circular caverns, the pillar space of 2∼3 times the cavern diameter is only applicable to the case of low working pressure. Under high working pressure, the plastic strain area of the two caverns overlaps, which is not conducive to the safety and stability of the caverns. When the working pressure is greater than 16 MPa, a pillar space that is 4 times the cavern diameter is more appropriate.
3) The cavern diameter will significantly affect the mechanical response of the surrounding rock: with the increase in the cavern diameter, the maximum deformation of surrounding rock increases rapidly.

Acknowledgements

The authors gratefully acknowledge the support provided by China Energy Engineering Corporation Limited (No. CEEC2021-KJZX-04).

Conflict of interest

The authors declare no competing interest.

References

Jafarizadeh, H., Soltani, M., Nathwani, J. Assessment of the Huntorf compressed air energy storage plant performance under enhanced modifications. Energy Conversion and

Management, 2020, 209: 112662.

Jiang, Z., Li, P., Zhao, H., et al. Experimental study on performance of shallow rock cavern for compressed air energy storage. Rock and Soil Mechanics, 2020, 41(1): 235-241. (in Chinese)

Kim, C., Chen, L., Wang, H., et al. Global and local parameters for characterizing and modeling external corrosion in underground coated steel pipelines: A review of critical factors. Journal of Pipeline Science and Engineering, 2021, 1(1): 17-35.

Kushnir, R., Dayan, A., Ullmann, A. Temperature and pressure variations within compressed air energy storage caverns. International Journal of Heat and Mass Transfer, 2012, 55(21-22): 5616-5630.

Leis, B. Evolution of metal-loss severity criteria: Gaps and a path forward. Journal of Pipeline Science and Engineering, 2021, 1(1): 51-62.

Lund, H., Salgi, G. The role of compressed air energy storage (CAES) in future sustainable energy systems. Energy Conversion and Management, 2009, 50(5): 1172-1179.

Marcus, B., Daniel, W., Roland, S., et al. A review on compressed air energy storage: Basic principles, past milestones and recent developments. Applied Energy, 2016, 170: 250-268.

Peng, W., Shang, H., Ji, W., et al. Key process of artificial chamber siting for compressed air energy storage power plant. Electric Power Survey and Design, 2023, 180: 46-49. (in Chinese)

Rutqvist, J., Kim, H., Ryu, D., et al. Modeling of coupled thermodynamic and geomechanical performance of underground compressed air energy storage in lined rock caverns. International Journal of Rock Mechanics and Mining Sciences, 2012, 52: 71-81.

Serbin, K., Slizowski, J., Urbanczyk, K., et al. The influence of thermodynamic effects on gas storage cavern convergence. International Journal of Rock Mechanics and Mining Sciences, 2015, 79: 166-171.

Wan, J., Meng, T., Li, J., et al. Energy storage salt cavern construction and evaluation technology. Advances in Geo-Energy Research, 2023, 9: 141-145.

Wan, J., Sun, Y., He, Y., et al. Development and technology status of energy storage in depleted gas reservoirs. International Journal of Coal Science & Technology, 2024, 11: 29.

Wang, F., Wang, H., Wu, M., et al. Compressed air energy storage technology and development. Hydropower Generation, 2022, 48(11): 10-15.

Xia, C., Zhang, P., Zhou, S., et al. Stability and tangential strain analysis of large-scale compressed air energy storage cavern. Rock and Soil Mechanics, 2014, 35(5): 1391-1398. (in Chinese)

Zhou, S., Xia, C., Du, S., et al. An analytical solution for mechanical responses induced by temperature and air pressure in a lined rock cavern for underground compressed air energy storage. Rock Mechanics and Rock Engineering, 2015, 48(2): 749-770.

Zimmels, Y., Kirzhner, F., Krasovitski, B. Design criteria for compressed air storage in hard rock. Energy and Environment, 2002, 13(6): 851-872.